AIAA−2003−0418

EXPERIMENTAL INVESTIGATION OF THE AERODYNAMIC CHARACTERISTICS OF FLAPPING−WING MICRO AIR VEHICLES

K.D.Jones and M.F.Platzer

Naval Postgraduate School
Monterey, CA

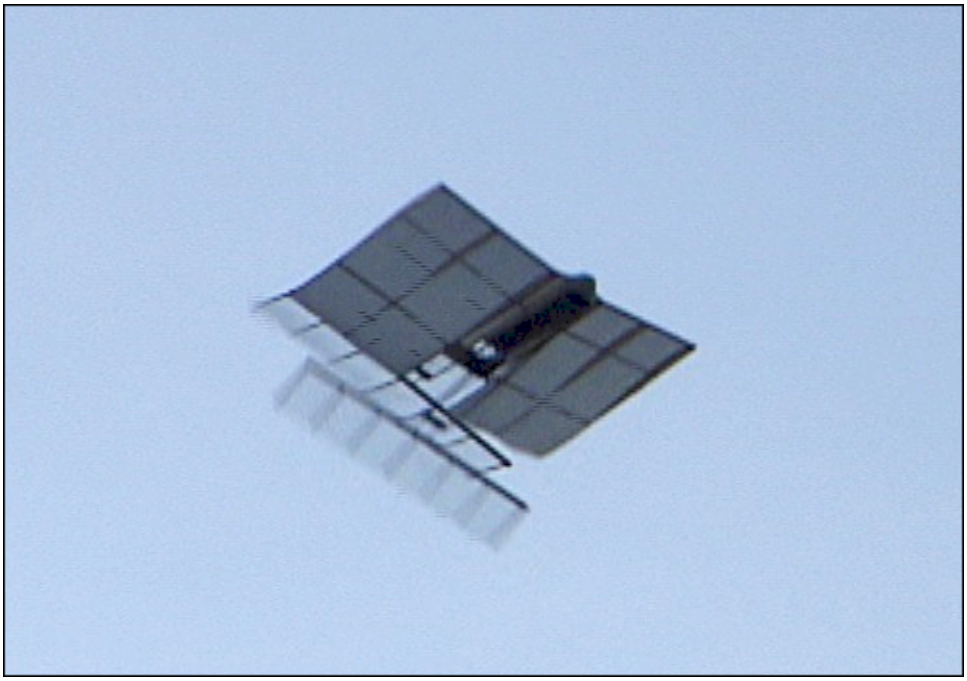

41st Aerospace Sciences Meeting & Exhibit
6−9 January 2003 / Reno, NV

EXPERIMENTAL INVESTIGATION OF THE AERODYNAMIC CHARACTERISTICS OF FLAPPING-WING MICRO AIR VEHICLES

Kevin D. Jones[†] **and Max F. Platzer**[‡]

Naval Postgraduate School
Monterey, California

Abstract

In this paper the development and flight testing of a radio-controlled micro air vehicle propelled by flapping wings is described. The vehicle consists of a 30cm-span, 14.5cm-chord fixed-wing, with two flapping wings immediately downstream of the fixed-wing. The flapping wings, with a 25cm-span and 4cm-chord, are arranged in a biplane configuration and flap in counterphase, providing a mechanically and aerodynamically balanced platform. Flight tests have shown that the configuration is particularly well suited for low speed flight, due to the inherent resistance to flow separation facilitated by flow entrainment from the flapping wing pair. The 14 gram model has demonstrated stable flight at speeds between 2 and 5m/s, and the model exhibits a very rapid stall recovery under power, due to the flow entrainment effect.

Nomenclature

c = chord length
C_L = lift coefficient, lift$/(q_\infty S)$
C_M = moment coefficient, moment$/(q_\infty cS)$
C_P = power coef., power$/(q_\infty SU_\infty) = -C_L\dot{z} - C_M\dot{\alpha}$
C_T = thrust coef., thrust$/(q_\infty S)$
f = frequency in Hertz
h = plunge amplitude in terms of c
k = reduced frequency, $2\pi fc/U_\infty$
q = dynamic pressure, $\rho U^2/2$
Re = chord Reynolds number, $U_\infty c/\nu_\infty$
S = wing area
t = time
U_∞ = free-stream velocity
x, z = Cartesian coordinates in terms of c
α = angle of attack
η = propulsive efficiency, $\overline{C_T}/\overline{C_P}$
ν = kinematic viscosity
ρ = density
τ = nondimensional time, tU_∞/c
$(\dot{})$ = rate of change with respect to τ
$(\bar{})$ = averaged over one period
$(\,)_\infty$ = free-stream value

Introduction

The agile flight of birds and insects has been an inspiration to scientists for many centuries. However, since the first part of the 20th century, little effort has been directed toward understanding and exploiting the aerodynamics demonstrated by these creatures. The lack of industrial applications has relegated the study of flapping-wing flight to something of a *hobby-like* status, with very little research funding available for dedicated scientific investigations, such that most notable progress has been made by model airplane enthusiasts.

However, recent interest in small, unmanned air vehicles (UAVs) and micro air vehicles (MAVs) has led to a renewed interest in flapping-wing propulsion, and an influx of research funds. The ability of the dragonfly to hover and maneuver in confined areas, as well as to achieve high speeds and to fly in turbulent air has drawn significant interest, but has as yet proved to be a formidable goal for scientists to duplicate numerically or experimentally.

While flapping-wing model aircraft are not new, dating back at least to 1874, when Alphonse Penaud built a rubber-band powered ornithopter, with just a few exceptions, almost all successful flapping-wing aircraft have been based on a bird-like morphology, at least for the flapping-wings. Presumably the popularity of bio-mimicry is based on an assumption that evolution has weeded out all of the unsuccessful designs, leading to the belief that what is left is the definitive optimum.

While one cannot easily argue against the principle of optimization inherent in an evolutionary process, one must also consider the initial conditions and constraints of the process. For example, the fact that no living creatures use a rotating propeller to fly is not proof that flapping-wings are superior. Rotating parts are just not all that common in organic creatures. Likewise, it is pretty rare for a four-legged creature to sprout a new pair of appendages for some new purpose. It is much more common to just reassign the purpose of the existing appendages (i.e., fins-to-feet, arms-to-wings, etc.). That being said, much can be learned from observations of nature and, in fact, there are many successful flying vehicles that use bird-like flapping, but usually with more conventional tails.

[†] Research Associate Professor, Senior Member, AIAA

[‡] Professor, Fellow, AIAA

Probably the most publicized bio-mimetic flapper is AeroVironment's *Microbat*. While the Microbat has appeared in countless popular magazines (e.g., Ref. 1), the only publications in the scientific literature that we are aware of relate to the MEMs construction of wings (e.g., Pornsin-Sisirak *et al*[2]). There the radio controlled vehicle is described as having a 23cm span and 12.5g weight, and requiring about 1.5W to fly. They reported a 42 second flight, limited by the available power from the NiCd battery. Information posted on the web reports that a later version with PLiON batteries achieved a flight of over 6 minutes (touch.caltech.edu/research/bat/bat.html).

Projects like the Microbat clearly demonstrate that mimicking bird morphology can lead to success, but one is left to ponder whether or not there is a better way. For example, model airplane enthusiasts have been building rubber-band powered ornithopters for more than a century, and to date, the greatest duration was achieved by something that did not look at all like a bird, using instead a biplane flapping mechanism, as shown in Fig. 1. The biplane or *X-wing* canard flapper, built in 1985 by Frank Kieser, set a new record for indoor freeflight duration.[3] Variations of this design still hold the record.

A collaboration between SRI and the University of Toronto has developed the *Mentor*, a 30cm-diameter, 450g vehicle that can reportedly hover under its own power.[4] Like Frank Kieser's design, the Mentor is designed to capitalize on the Weis-Fogh or *clap-and-fling* effect, and seems to be designed specifically for hovering flight - a flapping-wing helicopter of sorts. Both deigns exploit a facet of animal flight technique, the Weis-Fogh effect, but they do it in a way that is quite different than we see in nature; going one step further than just mimicking nature.

It is often instructive to observe how animals have adapted their behavior to compensate for biological constraints. For example, birds have evolved with a single pair of wings, so configurations such as the model shown in Fig. 1 are not possible. However, observations of bird flight low over the ocean indicate that birds have indeed discovered the benefits of flapping in ground effect, and it is this behavioral adaptation that is exploited in this investigation.

This paper summarizes the authors' work over the last decade, ultimately leading to the development of radio-controlled flapping-wing micro air vehicles with a very unconventional configuration. In pursuing this goal, the following design and development philosophy was applied. First, it was realized that insufficient information was available about the aerodynamic characteristics of flapping wings at low Reynolds numbers. In particular, it was unclear whether inviscid

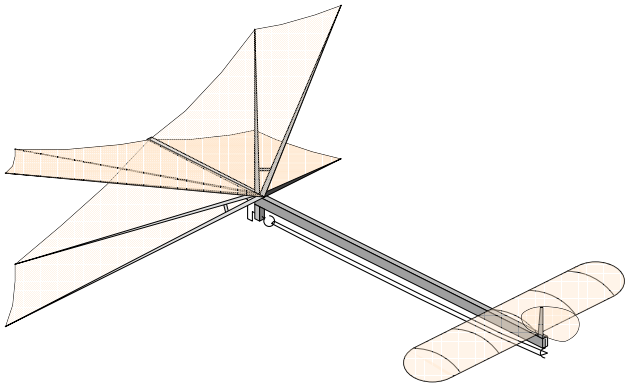

Fig. 1: 1985 record winning biplane ornithopter design.

flow theory would be capable of predicting these characteristics. Therefore, flow visualization experiments were performed to determine the dependence of vortex shedding from sinusoidally plunging airfoils on plunge amplitude and frequency, and the experimental observations were compared with the predictions from an unsteady panel code.

Second, an unconventional flapping-wing propeller developed in the 1940s by Wilhelm Schmidt (discussed in more detail in the next section) suggested the existence of favorable wake interference effects, making it advisable to perform a systematic exploration of configurations which might exploit this. Therefore, a wind tunnel model was constructed, and the thrust of oscillating tandem and biplane configurations was measured.

Third, it was argued that following bird morphology too closely was unwise, for several reasons. The flapping amplitude of bird wings varies along the span resulting in a highly three-dimensional flowfield, with the inner part of the wings contributing very little to the thrust generation. In contrast, by flapping the wing with a constant amplitude along the span, three-dimensionality would be reduced, and the inner portion of the wing would be more effective.

These considerations suggested the use of high-aspect-ratio flapping wings in a biplane configuration because of their favorable interference effect on thrust generation and the avoidance of dynamic imbalance effects. Finally, a close-coupled stationary wing and a biplane flapping-wing configuration was selected because of the favorable entrainment and, therefore, flow separation-control effect caused by the flapping wings immediately downstream of the stationary wing.

In the following sections, more justification for the unusual configuration is given, the qualitative and quantitative data from previous publications is summarized, and the trials and tribulations overcome to achieve a flying vehicle are presented.

Background

Throughout the past century, there have been a number of scientific contributors to the knowledge and understanding of flapping-wing flight. For brevity, we refer to Jones *et al.*[5] for a historical perspective of much of the past work, with only the present authors' contributions summarized here, along with a few additional references as needed.

Our work in flapping-wing propulsion began in the early-1990's when codes developed primarily for aeroelastic analyses were applied to the study of propulsion, and comparisons were made with water-tunnel experiments.[6] As any unsteady aerodynamicist should know, the difference between flutter and propulsion is a very small one. In fact, this was noted back in the 1920's by Birnbaum, a student of Prandtl, who developed the first analysis of flapping-wing propulsion and flutter.[7] In the 1930's Garrick developed a more comprehensive theory, based on Theodorsen's aeroelastic analysis to compute the streamwise forces.[8] In 1997, we explored some of the vast parameter space, noting the conditions that would lead to propulsion or power-extraction and, of particular interest, identifying the benefits of flapping near a ground plane.[9]

In the following years, more work was done to investigate configurations involving wake-interference, such as those depicted in Fig. 2. The first is the simple wing, the second is a model of Schmidt's *wave-propeller*,[10] a configuration where the stationary trailing airfoil generates *free* propulsion due to interference from the oscillatory wake of the leading airfoil, and the third is a biplane case, where two wings flap symmetrically in counterphase, emulating a single flapping wing near a ground plane.[11]

The time-averaged thrust coefficient and propulsive efficiency predicted by an unsteady panel code are shown in Figs. 3 and 4 for the three configurations. In all cases a NACA 0014 airfoil was oscillated sinusoidally in pure plunge, with a plunge amplitude of 0.4c, with $x_0 = 2.2$ for case (b), and $z_0 = 1.4$ for case (c). The values plotted for cases (b) and (c) are average values for the two wings. The forward airfoil produces almost all of the thrust in case (b), but both airfoils perform equally in case (c).

Garrick's theory was only applicable for the single-wing case, and the agreement with the panel code was quite good at low frequencies, degrading at higher frequencies. It was shown that the primary deficiency of Garrick's theory is the inability to model out-of-plane vorticity. If the panel code wake model is modified to emulate Garrick's wake model, then the two codes agree extremely well for all frequencies.

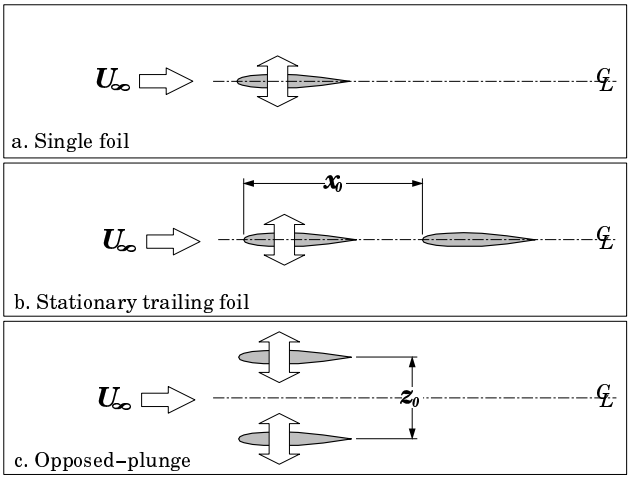

Fig. 2: Numerical and experimental configurations investigated.

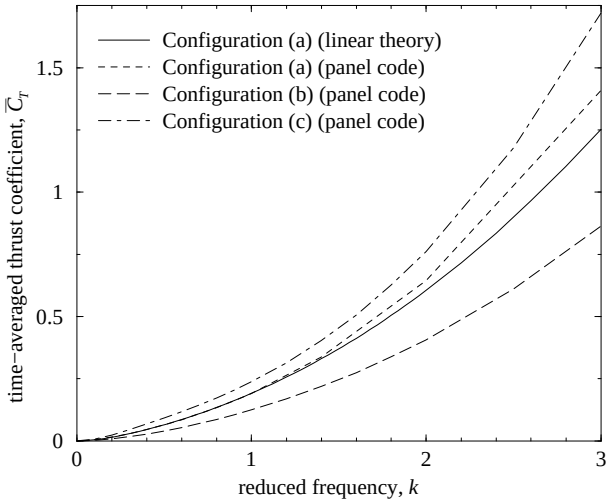

Fig. 3: Thrust coefficient versus reduced frequency.

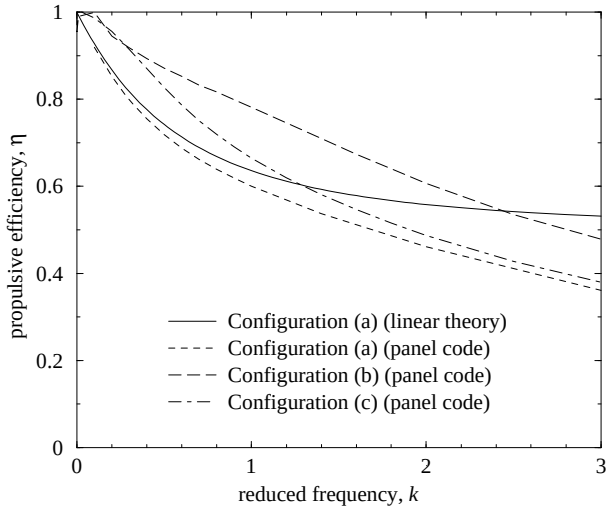

Fig. 4: Efficiency versus reduced frequency.

Observations of bird flight over water confirm that the birds know about the benefits of flapping near a ground plane, as they often cruise so low that their wing-tips break the surface at the bottom of their flapping stroke.

While case (b), the *wave-propeller*, was found to produce the highest efficiency over the full frequency range, it was noted that due to the much lower average thrust coefficient, viscous losses, which are not considered in the panel-code solutions, would greatly reduce overall performance, particularly at lower Reynolds numbers where profile drag is relatively high. On the other hand, case (c), the biplane or ground-effect case, produced roughly double the thrust of (b), and still at a higher efficiency than (a). Case (c) offered the additional benefit of being mechanically and aerodynamically balanced and, therefore, for a flying vehicle, work would not be done flapping the fuselage.

These considerations led us to the construction and wind-tunnel testing of the model shown in Fig. 5, which would allow us to evaluate the integrity of the panel code predictions.[11] The model flapped two high aspect-ratio wings sinusoidally, with a maximum amplitude of $h = 0.4$. The wings had an airfoil section resembling a NACA 0014, with a 64mm chord, and an effective span of 1200mm. Flapping frequencies up to about 8 Hz were possible. To measure thrust, the model was suspended from the tunnel ceiling on four thin cables, as shown in Fig. 6, such that it could swing freely in the flow-direction but remained stable in all other directions. Thrust was determined by measuring the streamwise displacement of the model using a laser range finder.

The experiments were performed in the Naval Postgraduate School low-speed wind-tunnel, illustrated in Fig. 7, a continuous, flow-through facility with an approximate flow-speed range between 0 and 10 m/s. The measured thrust for a range of flow speeds and flapping frequencies is shown in Fig. 8, with the velocities corrected by Lund.[12] The agreement with the panel code was quite reasonable, especially considering that the experimental Reynolds numbers were between about 1.0×10^4 and 4.5×10^4. In particular, the trend toward increasing thrust with increasing flow-speed was encouraging.

In the following years the biplane configuration evolved into a flapping-wing design for MAVs, such as the propulsive test model shown in Fig. 9.[12–15] The MAVs were designed around the DARPA criteria, limiting them to a 15cm length and span. They had weights between about 6 and 10g, and the tiny stepping motors could drive them up to flapping frequencies of about 40Hz.

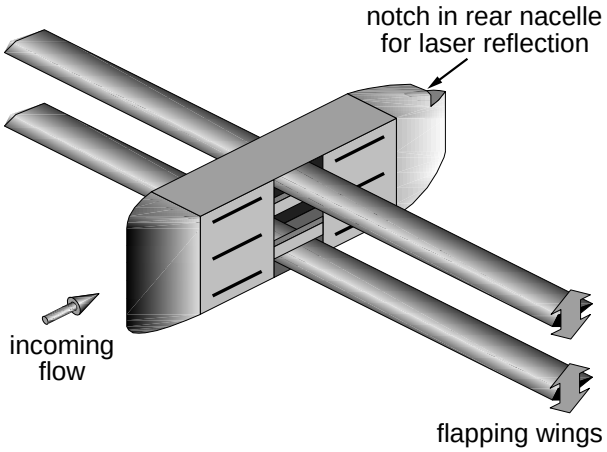

Fig. 5: Isometric view of the large model.

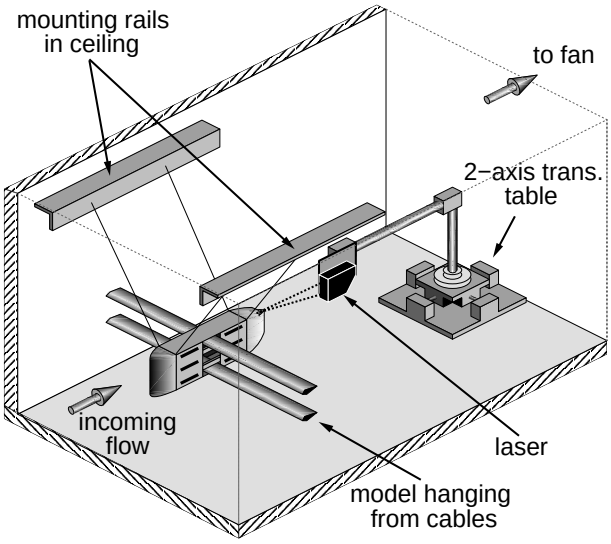

Fig. 6: View of the large model in the test-section.

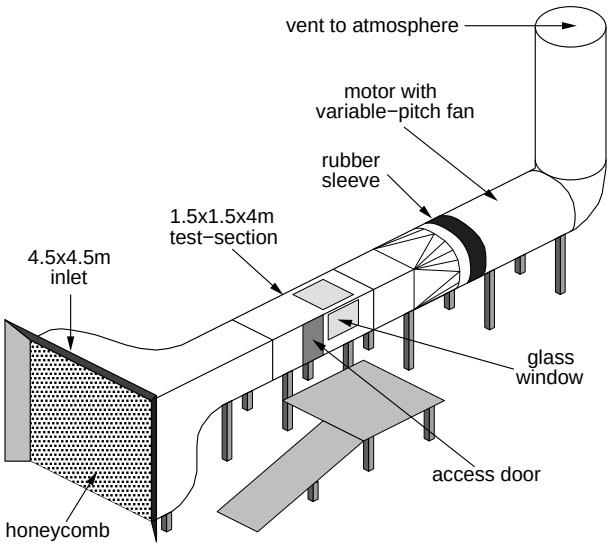

Fig. 7: Schematic of the NPS low-speed wind tunnel.

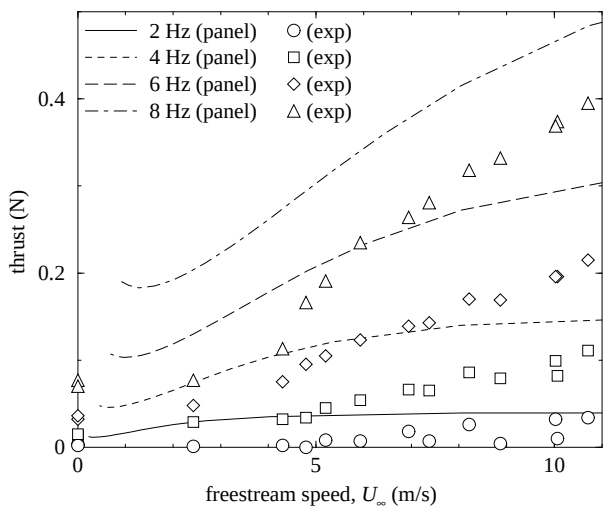

Fig. 8: Measured and predicted thrust for the large model.

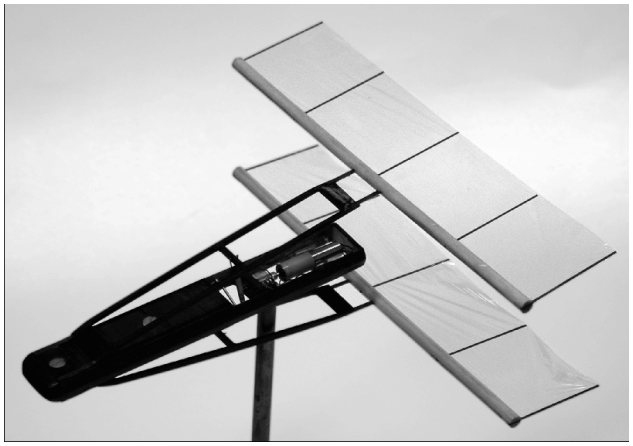

Fig. 9: Typical 15 cm length/span MAV propulsion model.

Thrust for the MAVs was measured in a similar way to the larger model, but the support cables were replaced with 0.125mm diameter, single-strand, bare copper wire. As well as supporting the model, the wires were used to power the motor, with three of the wires going to the three poles on the stepping motor, and the fourth providing a back-EMF signal for the closed-loop motor controller.

Typical performance of a MAV is shown in Fig. 10, and contrary to what was found for the large model, the MAV performance decreased rapidly with velocity. This was partially due to a passive feathering mechanism which must be tailored to a specific speed, but it was also thought that flow separation played an important role in this behavior. To investigate this, in a follow-on study low Reynolds number Navier-Stokes simulations of the large model were performed.[16–19] Simulations of a stationary airfoil at Reynolds number 10^4 predicted periodic shedding with $k \approx 12.3$, and experimental measurements using a strobe light showed similar behavior with $k \approx 14.5$, as shown in Fig. 11.

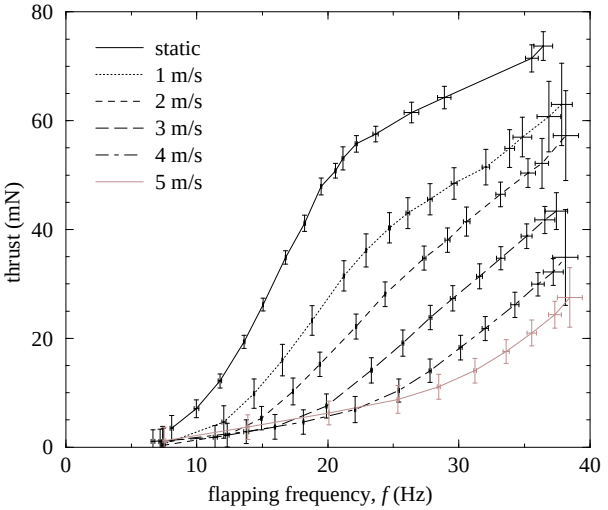

Fig. 10: Measured thrust for a typical MAV model.

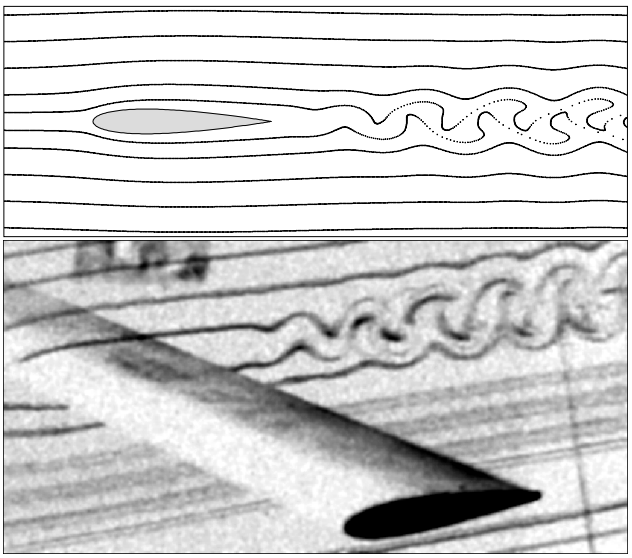

Fig. 11: Numerical and experimental streaklines for Re=10,000.

The Reynolds number dependence of thrust production is shown in Fig. 12. The agreement between the panel code and the high Reynolds number Navier-Stokes simulations was excellent, even at frequencies where the induced AOA greatly exceeded the static stall angle (> 30 degrees). A significant reduction in performance was predicted in the low Reynolds number simulations throughout the frequency range. The experimental results, with $0.5 \times 10^4 <$Re$< 4.5 \times 10^4$, filled the gap between the high and low Reynolds number Navier-Stokes simulations and demonstrated a consistent trend.

Unfortunately, while the low Reynolds number simulations appeared to agree well with experiments on the large flapping model, numerical capabilities still fell short of being able to handle the complexities of the MAV models. Assumptions of two-dimensional flow

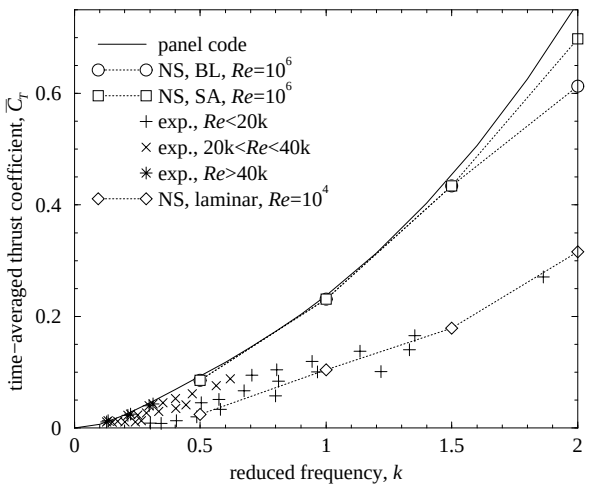

Fig. 12: Predicted and measured thrust for the large flapper.

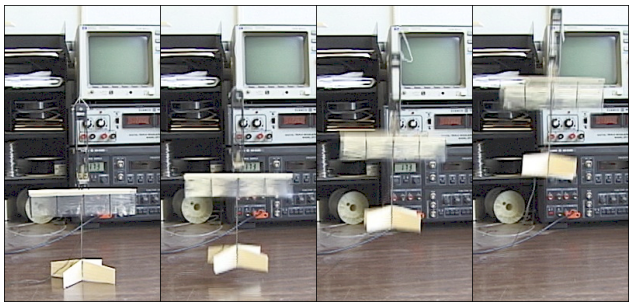

Fig. 13: Vertical takeoff MAV.

were demonstrably inappropriate, and the aeroelastic behavior of the flexible wings and the passive aeroelastic pitching motion increased the complexity of the simulations considerably. Therefore, as detailed in the remainder of the paper, the investigation evolved into a purely experimental project.

Development of a Flying Vehicle

With the knowledge that the flapping-wings would ultimately be most effective for low speed or perhaps hovering flight, the difficult task of integrating them into a complete vehicle was undertaken.

Vertical Take-Off

With a few iterations of manual optimization, a configuration was built that would produce over 14g thrust. The 9.5g model was fitted with tail fins to provide some stability, and vertical takeoff was demonstrated, as shown in the sequence of photos in Fig. 13. The VTO model still utilized the stepping-motors and, therefore, power was still fed in through trailing wires. Additionally, flapping in excess of 40Hz, the model was not very efficient but, nevertheless, demonstrated the lifting potential of the biplane configuration.

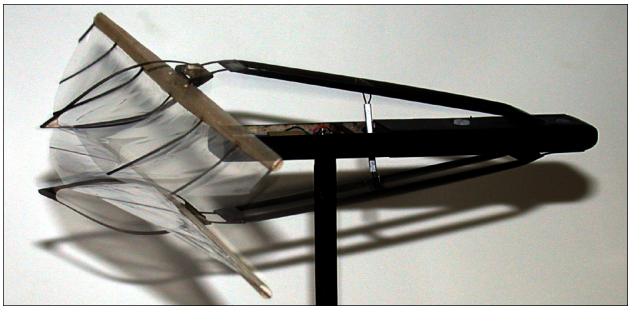

Fig. 14: Passive aeroelastic cambering wings.

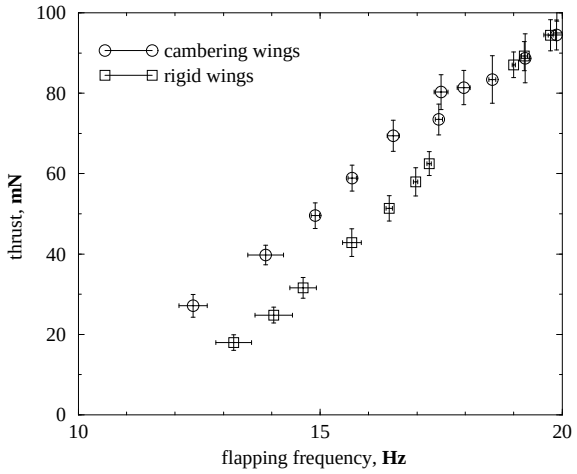

Fig. 15: Static performance of the cambering wings.

Passive Aeroelastic Cambering

While passive aeroelastic pitching had been utilized on all previous MAVs, the effect of passive aeroelastic cambering wings was now investigated. On the older wings, depending on the stiffness of the wing ribs, cambering would always occur under load, but in the wrong direction, deflected away from the load, and for lighter (more flexible) wings, higher-order harmonics showed up in the camber-line at higher frequencies, resulting in a rapid decrease in performance.

As shown in Fig. 14, the elastic cambering was performed by using flexible ribs or *batons* on the flapping wings attached to simply-hinged leading edge spars and constraining the camber-line at the wing centerline with a stiff but light carbon-fiber cage. While static tests showed improved performance at low flapping frequencies, the aeroelastic behavior deteriorated at higher frequencies, as shown in Fig. 15. Additionally, the cambering wings weighed more, were much more difficult to build and were more fragile. Consequently, they were only used on a few models, with most models using very rigid wing-ribs, which were reliable at all frequencies.

Lift Production

The unconventional flapping mechanism on our models essentially required that a complete vehicle would be a *pusher* and that fixed wings would be needed to get the center of lift closer to the center of mass. The first attempt at an integrated model, shown in Fig. 16, utilized a 15cm-span, reflexed fixed wing ahead of and centered between the flapping wings.

All previous models had utilized the very small, Smoovy stepping-motors with the compact, attached, 25:1 planetary gear reduction. However, in order to get sufficient power for the MAVs the stepping motors required an excess of 15 volts. Additionally, they were driven by a very large closed-loop controller that was not easily miniaturized for a flying model. Therefore, in the flying models, the stepping motors were replaced by tiny DC pager-motors, and custom gear drives were assembled using nylon gears from tiny wind-up toys, micro servos, and indoor-RC manufacturers.

The model shown in Fig. 16 used a 6mm diameter by 10mm long motor, with a 2 stage 22:1 gear drive using gears from tiny wind-up toys. The model weight without batteries was about 6.8 grams. In order to test the fragile model without risk of damaging it, we assembled a rotary-arm test stand which allowed the model to propel itself around a circular path, as shown in Fig. 17. The model was attached to the end of the rotating arm using a short pivoting fixture which provided for a means to assess lift. The model center of mass is at a 1m radius from the central pivot. Tests on the stand showed a maximum flight speed of about 3.5m/s at zero lift while running on 5 volts. At an angle of attack where lift≈weight (roughly 15 degrees), the flight speed was about 2.5m/s.

While the *pusher* arrangement created difficulties concerning stability and control, it was believed to offer a significant advantage with regard to separation control over the main wing. In a study by Platzer *et al*,[20] and a patent by Platzer[21] it was shown that the entrained flow ahead of a flapping wing could be used to prevent flow separation, even in strong adverse pressure gradients. Flow-visualization tests of the MAV seemed to confirm this, as seen in Fig. 18. In the left image, the flapping-wings are static, and massive separation from the leading edge of the main wing is apparent. In the right photo, with the wings flapping at about 20Hz, the flow is reattached.

Components of a Radio Controlled Vehicle

The first step in the design process was to assess the minimum weight requirements for propulsion, power and control. With a few exceptions, the equipment used is *off-the-shelf* (OTF) hardware available through the model aircraft industry.

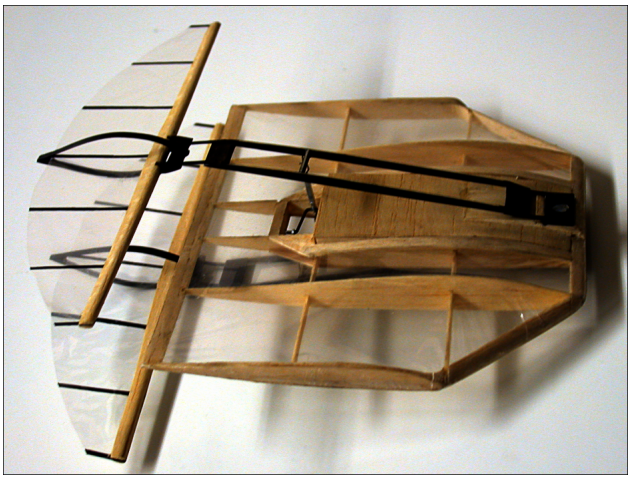

Fig. 16: First fixed/flapping-wing configuration.

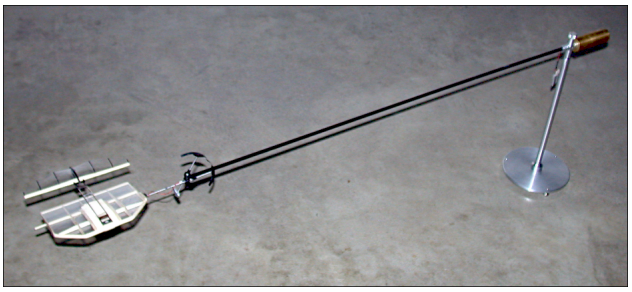

Fig. 17: Tethered flight on the radial-arm test stand.

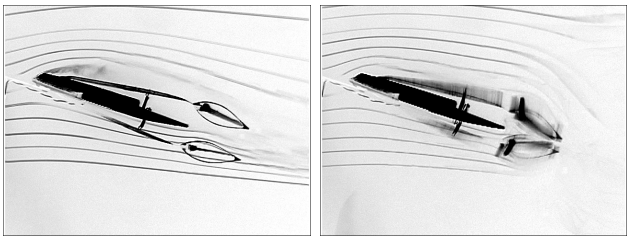

static dynamic

Fig. 18: Suppression of flow separation at high AOA.

The drive system for the MAVs has evolved continually, leading to the minimalist assembly shown in Fig. 19, with a 24:1 ratio. The nylon gears ride on tubular stainless steel bearings and shafts, with everything held in place by a balsa/carbon-fiber ply frame. The complete assembly, with a 6×15mm pager motor, gears, crankshaft and wiring weighs just under 2.7g. Under load the motor draws between 1 and 1.5W.

While the pager motors are typically designed to run on 0.8 to 1.2 volts, in order to get sufficient power for the MAVs we run them at 5 volts. Weight constraints generally limit the MAVs to a single battery cell, either NiCd, NiMH or Li-ion polymer, and the low voltage from the battery is stepped up to 5 volts using a custom-built DC/DC converter, like the prototype

shown in Fig. 20. The device, based on the MAX1674 chip from Maxim-IC, is 12×8×8mm in size, and weighs about 0.6 grams with plugs. The prototype is printed on very thick (1.6mm) PCB. On thinner board, the device should be under 0.4 grams. The device takes a 1.5 to 5 volt DC input, and supplies a regulated 5 volts, with low ripple and up to a several Watt load.

The current MAVs are powered by a rechargeable, Li-ion polymer cell, like the one shown in Fig. 21. The 3.6g cells nominally run at 3.7 volts, and have a 135mAh capacity (0.5 Watt hr), more than 8 times the energy density of comparable NiCd cells. The cells need to be handled carefully. The solder tabs are easily damaged, hence the reinforced plug on the pictured cell. Also, if the batteries are drained below 3 volts, they may never recover, and some care is needed in recharging them. With the reinforcement and plug, the battery weighs about 3.8g.

An RFFS-100 3-channel receiver with electronic speed control (ESC) (www.slowfly.com) is used for radio control. The units, shown in Fig. 22, could easily be more compact, but they weigh just under 2g, and provide proportional control with about 100m range. The receiver is designed to operate tiny voice-coil servos, like those shown in Fig. 23. Under a very small spring load, the 1g servos provide proportional control. These voice-coil servos are much heavier than we would like, so we are currently exploring the use of Shape Memory Alloy (SMA) wire for a much lighter control system.

From past experience, the flapping wings typically weigh between 0.3g and 0.6g each, depending on their size, and the flapping beams and connecting rods are typically about 1g for the set. While the weight of the fixed-wings and the remaining structure would be dependent on the size, a weight of about 3g was assumed. For a complete system, for the time being with just throttle control, everything added up to a flying weight of just over 14 grams. Keeping in mind the 2.5m/s speed of the earlier MAV, the 15cm length/span limit seemed to be too lofty a goal, requiring $C_l = 1.6$ for an aspect-ratio 1 wing at a Reynolds number of 2.6×10^4, which we were pretty sure we could not achieve. Therefore, for the time being, we relaxed the size constraint.

While little experimental data is available for low aspect-ratio wings in the 2×10^4 to 5×10^4 Reynolds number range, papers by Laitone[22] and Torres and Mueller[23] suggested that lift coefficients on the order of about 0.6 were possible with an L/D_{max} of around 5 on an aspect-ratio 2 wing. This indicated that a wing area of about 0.06m^2 was needed.

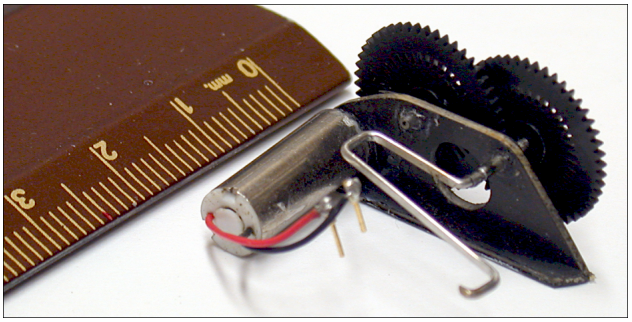

Fig. 19: 2.7-gram pager-motor/gearbox/crankshaft assembly.

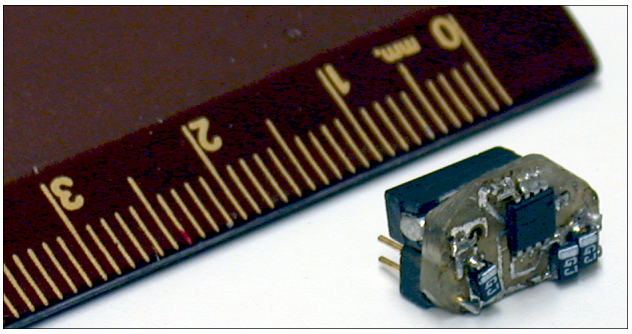

Fig. 20: 0.6-gram DC/DC converter.

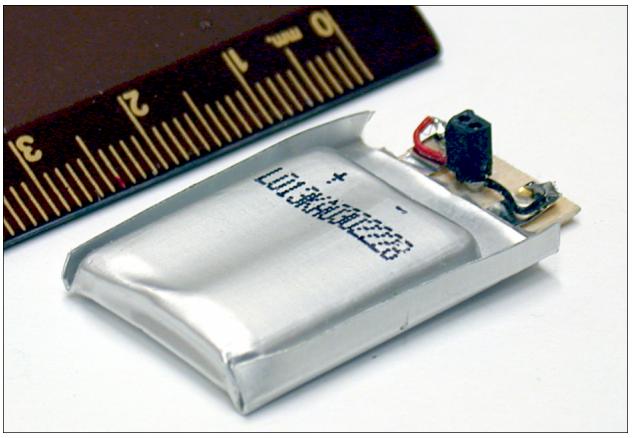

Fig. 21: 3.7 volt, 135mAh Li-ion polymer rechargeable battery.

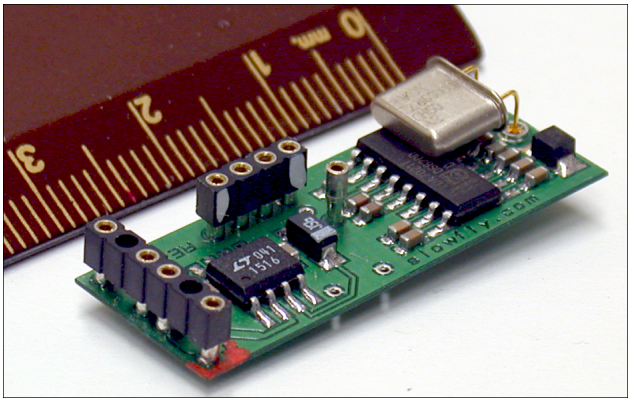

Fig. 22: RFFS-100 3-channel receiver/ESC.

Flying Model Design

After several design iterations the model shown in Figs. 24-27 was developed. It has a main wing with a 30cm span, 14.5cm chord, and a thin, reflexed airfoil. The flapping wings have a slightly shorter 25cm span, for added crash worthiness, and a 4cm chord. The model uses a positionable rudder and elevator for trim, with about 10 degrees of dihedral for yaw/roll stability. Since the current model has only throttle control, it is usually trimmed with a slight nose up attitude and a shallow left turn so that it remains in a relatively confined area. The complete model mass is about 14g, as detailed in Table 1.

Table 1: Mass Breakdown

Component	Mass
Motor/gear/crankshaft	2.66g
DC/DC converter	0.65g
Battery	3.76g
Receiver	1.95g
Antenna	0.08g
Wiring	0.13g
Flapping wings (pair)	1.30g
Flapping mechanism	1.10g
Main wing/fuselage	2.77g
Total	**14.40g**

While the ribs on the main wing have a thickness ratio of about 5%, the wing is only covered on the upper surface, so the reflexed airfoil is essentially infinitely thin, with the exception of a 4mm diameter half-round leading edge and a small tapered spar at about 0.3c. The reflex is needed to provide pitch-stability. The mean AOA of the flapping-wings is critical for trim, since they are the aft-most flying surface. Due to the lack of yaw and pitch controls in the present model, the flapping wings have been trimmed neutral, such that they do not change the pitch trim with power on/off. Test gliding the model from a hand launch shows an approximate L/D of 3, and this is fairly independent of the *at-rest* position of the flapping wings. If the flapping wings stop at the furthest apart position, there is a notable increase in drag.

The flapping wings have an amplitude of about 16.5mm ($h \approx 0.4$), and the flapping frequency can be adjusted remotely between zero and about 24Hz static, or just over 30Hz in flight. At 24Hz, the static thrust is about 9g, and the complete system draws about 1.5W. The ratio of grams-thrust to power-required is sometimes used as a figure of merit, in particular for hovering vehicles. This configuration gets about 6g/W. Some of our other models, with somewhat lower motor loads, have achieved over 7.5g/W.

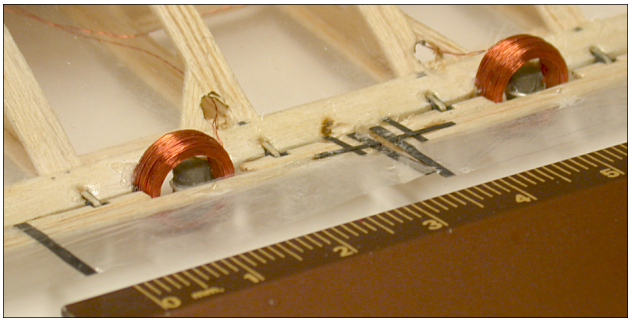

Fig. 23: 1-gram voice coil servos.

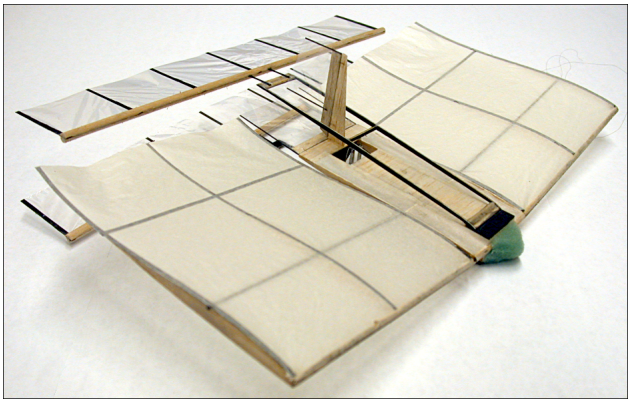

Fig. 24: 30cm-span radio control model.

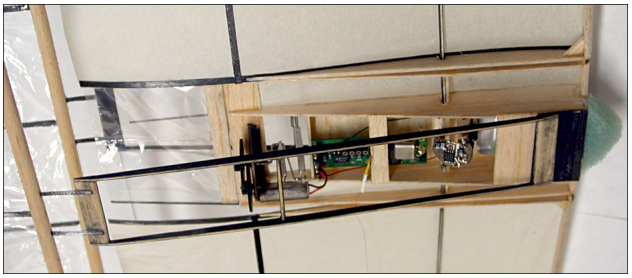

Fig. 25: Electronics package on the 14g model.

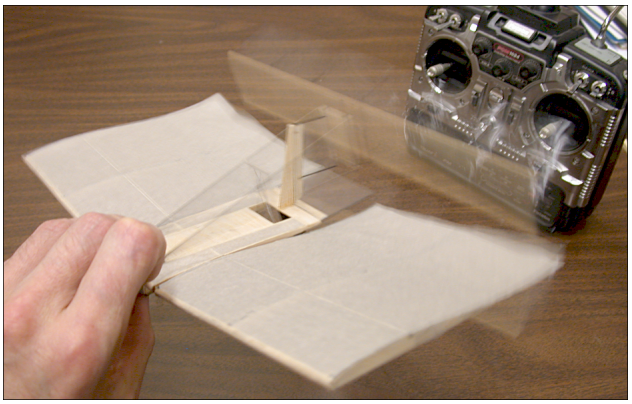

Fig. 26: Radio-controlled model in action.

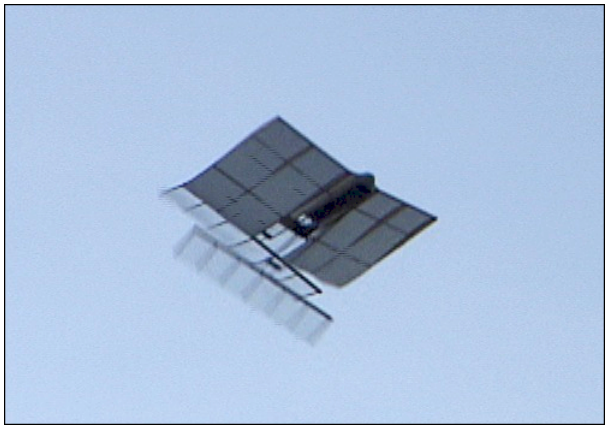

Fig. 27: Radio-controlled model in action.

According to the battery specifications, a 1.5W load should yield a flight time of about 20 minutes. While the longest recorded flight to date is just over 2 minutes, the duration is presently not limited by battery life, but rather by impact with solid objects, usually trees (recall that the current model has only throttle control). Flight speed is currently between about 2m/s and 5m/s, depending on the pitch trim. Due to the low flight speed, the model can turn within a 1m radius with minor deflections of the rudder making the design suitable for flight in confined areas. With a lack of in-flight pitch control, the model often experiences stall, either due to poor trimming, or to environmental perturbations. Due to the flow entrainment effect of the aft-placed flapping wings, stall recovery under power usually takes place in about one chord length. With power off, stall recovery may require a meter or more, depending on the stall depth.

Summary & Prospective

A radio controlled, 14 gram flapping-wing propelled micro air vehicle was developed and flight tested. The vehicle consisted of a 30cm-span, 14.5cm-chord fixed-wing, with two flapping wings immediately downstream of the fixed-wing. The flapping wings, with a 25cm span and 4cm chord, were arranged in a biplane configuration and flapped in counterphase, providing a mechanically and aerodynamically balanced platform. Flight tests have shown that the configuration is particularly well suited for low speed flight, due to the inherent resistance to flow separation facilitated by flow entrainment from the flapping wing pair. The 14 gram model has demonstrated stable flight at speeds between 2 and 5m/s, and the model exhibits very fast stall recovery under power, due to the favorable interference effect of the flapping wings.

Work is currently underway to integrate SMA or *muscle-wire* actuators for pitch and yaw control, and further miniaturization of the electronics is planned.

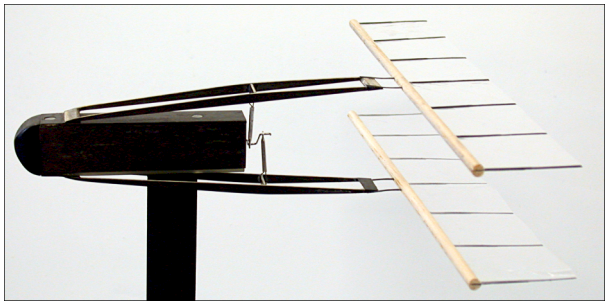

Fig. 28: Modular wind-tunnel model.

Fig. 29: Two-component force-balance for MAV loads.

Some weight reductions are immediately available, as battery weights have dropped from 3.6g to just under 3g, just in the last few months. Lower weights and component miniaturization will lead to reductions in the overall size of the MAV.

Two graduate students are currently working with the modular wind-tunnel model shown in Fig. 28 to further optimize the flapping-wing performance and the fixed/flapping-wing integration. Direct thrust and lift measurements will be made using a new two-component force balance, shown in Fig. 29, designed specifically for the very low forces encountered with these micro air vehicles. Additionally, flow visualization data will be obtained using a smoke wire, aiding in the quantification of flow separation and reattachment. The flapping-wing model incorporates an optical sensor to provide a TTL signal for synchronization with a TSI two-component unsteady LDV system, and unsteady velocity data will hopefully aid in further characterization of the unsteady flowfields.

Acknowledgments

We are greatful for the support received from Richard Foch, head of the Vehicle Research Section of the Naval Research Laboratory and project monitors Kevin Ailinger, Jill Dahlburg and James Kellogg.

References

[1] Grossman, J., "The Buzzzz at Caltech, Something New in Southern California's Skies," Los Angeles Times Magazine, Dec. 10, 2000, p. 8.

[2] Pornsin-Sisirak, T. Tai, Y. C. Ho, C. M., and Keennon, M., "Microbat: A Palm-Sized Electrically Powered Ornithopter," *2001 NASA/JPL Workshop on Biomorphic Robotics*, Pasadena, CA, Aug. 14-16, 2000.

[3] Chronister, N., "Ornithopter Media Collection," published on the web at *indev.hypermart.net/rubber.html*, 2000.

[4] Bridges, A., "Flying Robots Create a Buzz," Monterey County Herald, July 28, 2002.

[5] Jones, K. D., Lund, T. C. and Platzer, M. F., "Experimental and Computational Investigation of Flapping Wing Propulsion for Micro-Air Vehicles," Chapter 16, AIAA Progress in Astronautics and Aeronautics, Vol. 195, Fixed and Flapping Wing Aerodynamics for Micro Air Vehicle Applications, Ed. T. Mueller, AIAA, Reston, VA, 2001, pp. 307-339.

[6] Jones, K. D., Dohring, C. M. and Platzer, M. F., "Experimental and Computational Investigation of the Knoller-Betz Effect," **AIAA Journal**, Vol. 36, No. 7, July 1998.

[7] Birnbaum, W., "Der Schlagflügelpropeller und die kleinen Schwingungen elastisch befestigter Tragflügel," **Zeitschrift für Flugtechnik und Motorluftschiffahrt**, Vol. 15, 1924, pp. 128-134.

[8] Garrick, I. E., "Propulsion of a Flapping and Oscillating Airfoil," NACA Report 567, 1936.

[9] Jones, K. D. and Platzer, M. F., "Numerical Computation of Flapping-Wing Propulsion and Power Extraction," AIAA Paper No. 97-0826, Jan. 1997.

[10] Schmidt, W., "Der Wellpropeller, ein neuer Antrieb fuer Wasser-, Land-, und Luftfahrzeuge," Z. Flugwiss. Vol. 13, 1965, pp. 472-479.

[11] Jones, K. D. and Platzer, M. F., "An Experimental and Numerical Investigation of Flapping-Wing Propulsion," AIAA Paper No. 99-0995, Jan. 1999.

[12] Lund, T. C., "A Computational and Experimental Investigation of Flapping Wing Propulsion," Master's Thesis, Dept. of Aeronautics and Astronautics, Naval Postgraduate School, Monterey, CA, March 2000.

[13] Jones, K. D. and Platzer, M. F., "Flapping-Wing Propulsion for a Micro Air Vehicle," AIAA Paper No. 2000-0897, Jan. 2000.

[14] Jones, K. D., Duggan, S. J. and Platzer, M. F., "Flapping-Wing Propulsion for a Micro Air Vehicle," AIAA Paper No. 2001-0126, Jan. 2001.

[15] Duggan, S. J., "An Experimental Investigation of Flapping Wing Propulsion for Micro Air Vehicles," Master's thesis, Dept. of Aeronautics and Astronautics, Naval Postgraduate School, Monterey, CA, June 2000.

[16] Jones, K. D., Castro, B. M., Mahmoud, O. and Platzer, M. F., "A Numerical and Experimental Investigation of Flapping-Wing Propulsion in Ground Effect," AIAA Paper No. 2002-0866, Reno Nevada, Jan. 2002.

[17] Jones, K. D., Castro, B. M., Mahmoud, O., Pollard, S. J., Platzer, M. F., Neef, M., Gonet, K. and Hummel, D., "A Collaborative Numerical and Experimental Investigation of Flapping-Wing Propulsion," AIAA Paper No. 2002-0706, Reno Nevada, Jan. 2002.

[18] Castro, B. M., "Multi-Block Parallel Navier-Stokes Simulation of Unsteady Wind Tunnel and Ground Interference Effects," Ph.D. thesis, Dept. of Aeronautics and Astronautics, Naval Postgraduate School, Monterey, CA, Sept 2001.

[19] Mahmoud, O. M. K. M., "Experimental Investigation of Low Speed Flow over Flapping Airfoils and Airfoil Combinations," Ph.D. thesis, Dept. of Aeronautics and Astronautics, Naval Postgraduate School, Monterey, CA, Sept 2001.

[20] Platzer, M. F., Lai, J. C. S. and Dohring, C. M., "Flow Separation Control by Means of Flapping Wings," *Proceedings of the International Symposium on Seawater Drag Reduction*, Newport, RI, July 1998, pp. 471-478.

[21] Platzer, M. F., "Integrated Propulsion/Lift/Control Systems for Aircraft and Ship Applications," United States Patent Number 5975462, Nov. 1999.

[22] Laitone, E. V., "Wind Tunnel Tests of Wings and Rings at Low Reynolds Numbers," Chapter 5, AIAA Progress in Astronautics and Aeronautics, Vol. 195, Fixed and Flapping Wing Aerodynamics for Micro Air Vehicle Applications, Ed. T. Mueller, AIAA, Reston, VA, 2001, pp. 83-90.

[23] Torres, G. E. and Mueller, T. J., "Aerodynamic Characteristics of Low Aspect Ratio Wings at Low Reynolds Numbers," Chapter 7, AIAA Progress in Astronautics and Aeronautics, Vol. 195, Fixed and Flapping Wing Aerodynamics for Micro Air Vehicle Applications, Ed. T. Mueller, AIAA, Reston, VA, 2001, pp. 115-140.